



Cellulose-based fabrics triboelectric nanogenerator: Effect of fabric microstructure on its electrical output

Rawiwan KHWANMING¹, Satana PONGAMPAI², Naratip VITTAYAKORN² and Thitirat CHAROONSUK^{1,*}

¹ Department of Materials Science, Faculty of Science, Srinakharinwirot University, Sukhumvit 23, 10110, Watthana, Bangkok, Thailand.

² Advanced Material Research Unit, School of Science, King Mongkut's Institute of Technology Ladkrabang, 10520, Bangkok, Thailand.

*Corresponding author e-mail: thitirat@g.swu.ac.th

Received date:

10 March 2023

Revised date

25 April 2023

Accepted date:

28 June 2023

Keywords:

Cellulose fabrics;
Fabric structure;
Triboelectric nanogenerator;
Textiles

Abstract

At present, fabric-based triboelectric nanogenerator (TENG) has been paid attention and developed for self-power generation systems with wearability for E-textiles, especially cotton. However, there are many commercial cellulose-based fabrics with different fiber characteristics and fabric structures that gain possibility to effect on TENG performance and has been underreported. This work presents the fabrication of the textile TENG by using four types of commercial cellulose-based fabrics as friction layer and compare the electrical output efficiency relating their molecular structure, fabric structure and surface morphology characteristics. As shown by the electrical output, though all fabrics can generate electricity for TENG device, nevertheless, the output signal is different because of their different total surface area of the fabric, affecting by different microstructure. The rayon fabric contains the smallest size fiber with highest surface area at the same woven structure. The obtained output voltage (V_{OC}) and current (I_{SC}) of ~ 23 V and ~ 13 μ A are ~ 1.8 times higher than most studied cotton fabric. This research demonstrated the importance of the microstructure and surface area of the fabrics that significantly affect TENG properties. The investigation in this work will useful and knowledgeable to select fabric materials before improving and using them for energy harvesting devices.

1. Introduction

With the rapid development of intelligent networks, the emergence of new products such as smart sensors, health monitor system, wireless portability and many kinds in wearable electronic devices are increasable growth to receive and transmit information for making easy life and leading human society into the Era of Artificial Intelligence of Things (AIoT). As the results of huge demand and growth of those, textile-based electronics, and its components, known as electronic textiles (E-textiles), have attracted surging interest in recent years [1]. Among the electronic components, a power supply system to drive electronic components is always required. However, the large size, heavy weight and complex operating system are still limited for comfortable use.

Today, mechanical energy harvesting technologies are being developed to convert mechanical energy from human touch and movement into electrical energy called a triboelectric nanogenerator (TENG) [2,3]. The electricity generated by TENG is sufficient to drive small electronic devices. Relying on the literature searching, all kinds of materials; polymers, ceramics, and metals can be applied for the TENG devices [4,5,6]. Nowadays, fabrics have received much attention in textile TENG because they can be developed to use in a variety of devices, especially clothes [7,8] such as nylon, polyester, polyethylene, etc., which are synthetic fabrics [9,10,11,12]. Currently, according to the concern about environmental friendliness and electronic waste, natural-based fabric becomes attention. Cotton, which is cellulose-

based fabric, is the major player in this category, mostly due to its abundant quantity and widespread production with reasonably priced [13]. Importantly, a high tendency of losing electrons by containing the plentiful hydroxyl (-OH) groups makes the cotton becomes positively charges when in contact-separation with other triboelectric materials [14]. According to research in 2019, Jeong and co-workers fabricated cotton as a contact layer for TENG by designing plain and twill woven on the fabric structure. Their cotton TENG generated output voltage (V_{OC}) of 1.59 and 12.47 V for plain and twill weave, respectively [15]. In the same year, cotton fabric was created as friction layer by weaving with different conductive threads to make high performance TENG. The output voltage and current were found to be 1.5 V and 0.3 μ A.cm⁻² [16]. Sahu *et al.* [17] collected and directly utilized laboratory waste for fabricating a laboratory waste-based TENG operating in vertical contact-separation mode. The electrical output of the laboratory waste based TENG comprising PET and cotton gives a voltage of ~ 30 V and a current of ~ 0.2 μ A. Even though the literature can confirm the using of cotton as a friction layer in TENG, however, its electrical output is not much. Many modification strategies have been therefore paid on the pristine cotton, especially modifying electrode by weaving, or even adding conductor materials to improve the electron transportation performances for utilizing in TENG. In 2019, Zhu *et al.* [18] developed the self-functional sock by hybrid integrating PEDOT: PSS-coated cotton. The coated cotton sock shows the voltage and current of 55 V and 2.3 μ A under contact separation.

Sangkhum and co-workers [19] created an efficient natural textile-based TENG assembly to a Cu fabric electrode by dip-coated in cyanoalkyl silane and fluoroalkyl silane. This method can increase the output voltage and output current of cotton from 35.73 V to 139.08 V. However, the current has not been much improved as compared to the current improvement. The current is still provided for 4.25 μA . Dudem and co-workers [20] reported a cotton textile modified with PANI by the in-situ polymerization method to fabricate the TENG for harvesting the energy from human movements. By contacting with the PTFE film, the highest V_{oc} and I_{sc} values could be improved from approximately zero to 120 V and 4.2 μA . In 2022, a wheel-disk-shaped cotton woven with fluorinated ethylene propylene film has been fabricated and can generate the maximum V_{oc} and I_{sc} of 82 V and 8.9 μA [21]. As can be seen from the previous research, although cotton can be applied as a contact layer in TENG, and its efficiency can be improved in a variety of electron transportation improving processes. However the performance of the pristine cotton in the device is still limited with only enough to drive the sensors [22]. That is probably because of the limitation of fabric materials itself, *i.e.*, the molecular structure and microstructure. However, by looking for the cellulose-based fabrics, they do not contain only cotton. Cellulose fabrics are diverse types that are available and easily found in the market or commercial. Basically, there are two main types of celluloses: (1) natural cellulose: cotton and linen; and (2) regenerated cellulose: rayon and tencel fabrics [23], which contains different fabric characteristic and have not been fully studied in the TENG.

This work proposes the utilizing of four types from commercial cellulose-based fabrics, including cotton, linen, rayon, and Tencel as a friction layer material for the textile TENG fabrication. The fabric electrical output efficiency is studied for comparison and found to be relative to their microstructure and surface area. By using modified fabric-glue/CNT, the rayon fabric shows the output voltage (V_{oc}) and current (I_{sc}) of ~ 23 V and ~ 13 μA that are higher than other fabrics at the same weaving structure. The working on cellulose based in this research could pave the way for developing textile TENG by offering the significance of materials selection and making great inspiration for enhancing the self-powered personal electronics in future.

2. Experimental

2.1 Optimizing materials

Commercial Cotton, Linen, Rayon, and Tencel were purchased from Bulliontex Company (Thailand). All chemicals, including Sodium Chloride (NaCl, ACS reagent 99%), Calcium Chloride (CaCl_2 , ACS reagent 99%), Sodium Carbonate (Na_2CO_3 , BioXtra 99%), Sodium Hydroxide (NaOH, ACS reagent 97%, Carlo Erba Reactifs SA), Sodium Sulfate (Na_2SO_4 , ACS reagent 99%), Acetic acid (glacial 100%), and nonionic surfactant were procured from Sigma-Aldrich (USA).

2.2 Preparation of cellulose-based fabrics

2.2.1 Desizing

The mixed chemicals were prepared for desizing by mixing 1 g of NaCl, 0.05 g of CaCl_2 , 0.1 g of nonionic surfactant and 0.5 g of amylase enzyme in 100 mL of water. 5 g of fabric was immersed in desizing solution at 100°C for 45 min. The fabrics were boiled in boiling water for 10 min, then rinsed with clean water and dry.

2.2.2 Scouring

The scouring solution was prepared by mixing 0.2 g of NaOH and 0.01 g of nonionic surfactant in 100 mL of water. 5 g of desized fabrics were immersed in scouring solution at 95°C for 1 h. Then the fabric was rinsed with water at normal temperature and dry.

2.3 The fabrication of triboelectric nanogenerator (TENG device)

In this work, the TENG device consists of two contact layers of cellulose-based fabrics and polytetrafluoroethylene (PTFE). The fabric contact layer is bonded by a conductive fabric electrode prepared by soaking the adhesive fabric in 0.15 g of CNT solution. An aluminum tape electrode attaches to the PTFE layer. The acrylic sheets were used to cover the top and bottom of the device to support each layer when measuring by fixing the gap between both sides with a spring as shown in Figure 1.

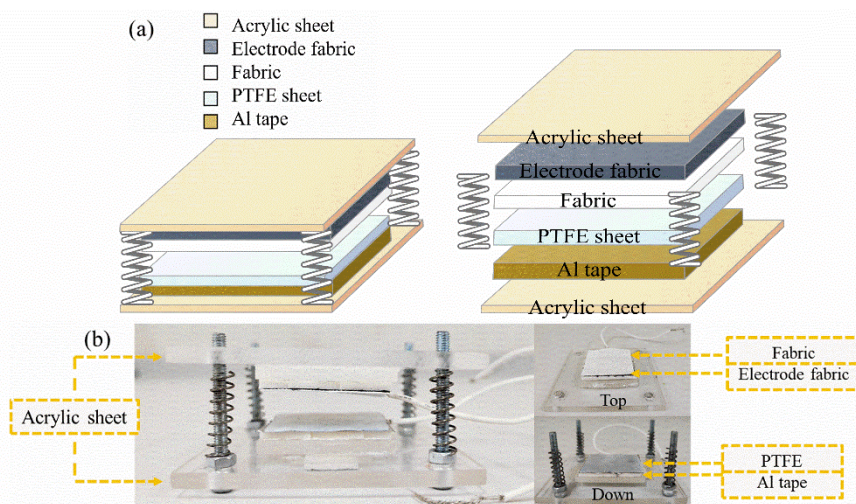


Figure 1. Structure and components of TENG by drawing (a) and real photographs of TENG device *via* digital camera (b).

2.4 Characterization and electrical output measurement

The morphology of all fabrics was analyzed by scanning electron microscopy (SEM, Quanta 250 model, USA). Surface and weaving structure of commercial cellulose-based fabrics were analyzed by digital camera and light microscopy. The functional groups were examined by Attenuated Total Reflectance Fourier Transform Infrared spectroscopy (ATR-FT-IR) model PerkinElmer/Universal-ATR from the USA. The electrical output performances of cellulose-based fabric TENG was measured by an oscilloscope (DSO-x 2012A, Keysight) and a digital multimeter (DMM, DM3058E, Rigol).

3. Results and discussion

3.1 Commercial cellulose-based fabrics characterizations

The fabric used in this work is based on the categorization of cellulose fabrics of natural cellulose fibers (Cotton, Linen) and regenerated cellulose fibers (Rayon, Tencel). Figure 2 shows the functional group identity of all commercial cellulose fabrics, showing the uniqueness of cellulose molecules. The absorption peak at 3330 cm^{-1} is attributed to the stretched vibration of the hydroxyl group, which is the primary functional group of cellulose. The peak at 2896 cm^{-1} is characteristic of the stretching vibration of C-H present in cellulose and hemicellulose. The absorption bands at 1360 cm^{-1} and 1315 cm^{-1} are relative to bending vibrations of the C-H and C-O groups of the aromatic rings in cellulose polysaccharides. At the peak position of 1051 cm^{-1} , the symmetric and asymmetric oscillation of the C-O-C bond is observed. And the peak at 894 cm^{-1} indicates the presence of β -glycosidic linkages between monosaccharides. Notably, IR spectra of regenerated cellulose at the absorption band of 1428 cm^{-1} , associated with the CH_2 symmetric bending of the cellulose were observed only in natural cellulose fibers. The regenerated cellulose fibers exhibited weaker peaks and shifted peaks to 1420 cm^{-1} formed by the fiber manufacturing process as corresponded to Comnea-Stancu *et al.* report [24,25]. The IR characteristics can confirm that all commercial fabrics are composed of cellulose as the main molecular structure. All those peaks correspond to the analyzed cellulose fabrics by Portella *et al.* and other literatures [26,27,28]. However, even though the main functional groups of all commercial fabric are similar, but the microstructure of the commercial fabric is different that directly effect to their electrical output efficiency. This point will be discussed later in the next part.

3.2 Morphological and physical properties of the cellulose-based fabrics

Figure 3 shows the zoom-in weaving structures of commercial cellulose-based fabrics by the digital camera. The result found that not all the commercial fabrics that show the same weaving structures. The structure of cotton, linen, and rayon fabric has similar weave structure, called the plain weave that is a weaving where the weft contrasts with the warp at perpendicular angles (graphic insert in Figure 3(a-c)). Tencel fabric is the only one that has a different weave structure of twill weave (Figure 3(d)). Twill weave is weaving with a diagonal pattern that is parallel to each other. The weft inserts it under

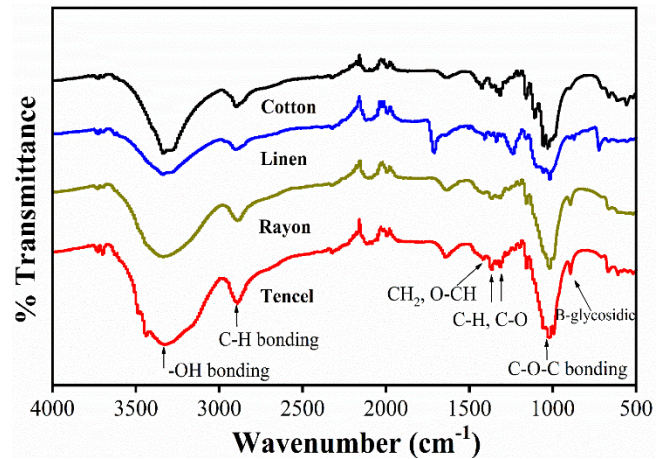


Figure 2. The functional group identification for the commercial cellulose-based fabrics by IR-ATR technique.

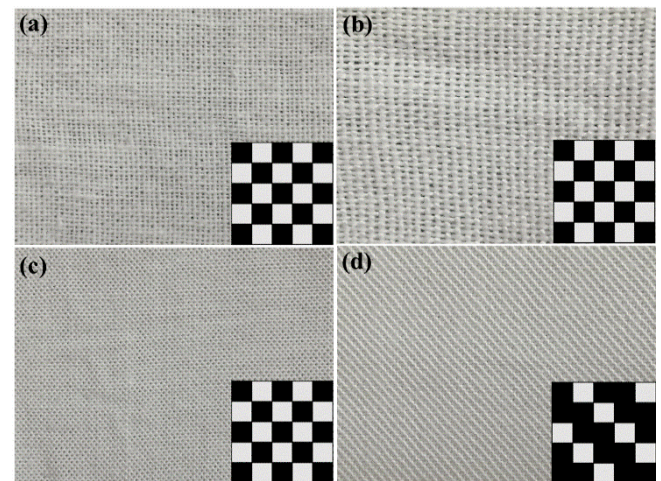


Figure 3. Photograph of commercial cellulose-based fabrics by digital camera; cotton (a), linen (b), rayon (c), and tencel (d).

two or more warps with steps between the rows to create a diagonal pattern (graphic insert in Figure 3(d)). As found by the literature, the different woven structures show a direct relationship with the surface area of the fabric, resulting in the difference output signal generated by TENG. In 2020, Somkuwar *et al.* [29] fabricated the textile fabric-based TENG using electrodes comprising types of woven fabrics of 1/1 plain weave and 5/1 twill weave. A maximum voltage output of 2.52 V was generated in a 1/1 plain weave and the 10.93 V was generated by a 5/1 twill weave fabric. The reason comes to the importance of contact area. In a plain structure, the contact area is mostly at the crossover points, resulting in scattered point contacts between the surfaces. The maximum output occurred in 5/1 twill comes from having of more regular and extended length of yarn contact area. As the surface area increases, and a larger surface charge is induced on the triboelectric layer. Consequently, the fabric woven structures can affect the electrical performance following the yarn weave pattern.

The SEM images clearly show the difference in the fiber morphology of the rayon, cotton, linen, and tencel fabrics. Figure 4(a) shows that the rayon fiber contained a lengthwise striated surface and bright with average diameter of about $18.8 \pm 6\ \mu\text{m}$. The cotton fiber (Figure 4(b)) has $21.8 \pm 8\ \mu\text{m}$ of average diameter with a ribbon shape and many

twists along its length. The twists of fiber give cotton a flat and uneven fiber surface. A characteristic of linen fiber is the presence of fiber nodes or joints that are small, soft, and irregular lumps with $25.6 \pm 11 \mu\text{m}$ of average diameter. The fiber nodes occur randomly along the length of the fiber as clearly illustrated by SEM Figure 4(c) of linen fibers. For the Figure 4(d) shows the longitudinal surface of tencel fiber that smooth and cylindrical with no striation. The average diameter of tencel was $19.3 \pm 7 \mu\text{m}$. By observing from the result, the rayon had lengthwise striated surface with smaller average diameter than those of other type cellulose fibers. Different average diameters will affect the different contact area of the fabrics in the means of using in TENG. Due to the small diameter fiber, rayon will probably contain more fiber per unit weight of the fabric and a high total surface area of fabric. To confirm this, the surface area of the fabric was calculated by measuring the size of the fabric divided by the weight of the fabric and calculated by the following:

$$\text{Surface area of fabric} = M^2/G \quad (1)$$

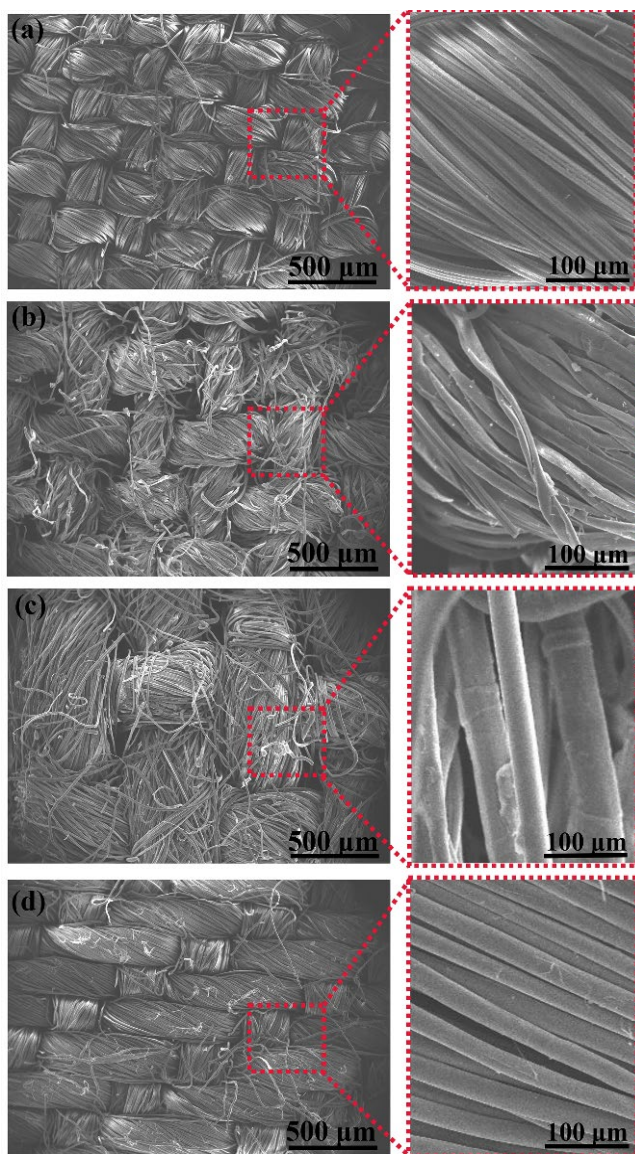


Figure 4. Surface morphology of cellulose-based fabrics; rayon (a), cotton (b), linen (c), and tencel (d) observed by SEM.

Where, M is the area of fabric (m^2) producing by measuring the width and length of the fabric, and G is weight of fabric (g). Therefore, the surface area is the accessible area of fabric surface per unit mass of fabric. The result of the total surface area for all commercial fabrics was found to be $0.0085 \text{ m}^2 \cdot \text{g}^{-1}$, $0.0054 \text{ m}^2 \cdot \text{g}^{-1}$, $0.0079 \text{ m}^2 \cdot \text{g}^{-1}$, and $0.0044 \text{ m}^2 \cdot \text{g}^{-1}$ for rayon, linen, cotton, and tencel, respectively. This can confirm that the rayon fabric shows the highest total surface area directly relating to the result of average diameters and microstructures of the fibers in the fabrics.

3.3 The electrical output performance of the cellulose-based fabric TENG

As shown in Figure 5(a), the electric generation mechanism of the TENG is based on the coupling effects between triboelectrification and electrostatic induction of two different electronegativity (EN) materials [2,30]. When two electrically neutral materials come into contact (i), cellulose fabric with low EN values donates electrons and creates positive charges on the fabric surface itself. PTFE film with higher EN values accepts electrons and creates negative charges on the surface. This charge-exchanging process occurs without electrons and current flows because the two materials remain in contact with charge balancing. When the material is separated (ii), the PTFE film induces positive charges on the Al electrode meanwhile the cellulose fabric induces negative charges on the Al electrode in its side. In this induction process, a charge imbalance causes electrons to flow from the negative to the positively charged electrode. So, electricity can be provided through the external load. While the material is still separate (iii), the electrons will completely flow until the charges are back to balance again. When the two materials come into contact again (iv), an inductive charge causes electrons to flow through the load from the opposite direction. Then, the full signal of the alternating current can be obtained.

The study of the electrical output of TENG devices from 4 types of cellulose-based fabrics including the output voltage (V_{oc}) and output current (I_{sc}) under the contact separation mode were reported in Figure 5(b-c) All commercial cellulose-based fabrics can generate electrical output signal by meaning of TENG. For in the same weaving structure, cotton, linen, and rayon showed the V_{oc} of 12.69 V, 17.46 V and 23.17 V, respectively with the I_{sc} of 9.48, 9.07, and 13.08 μA . The electrical output confirms that rayon fabric provides the highest electrical efficiency relating to their fiber morphology and contacting area as mentioned earlier. Rayon has the smallest diameter with highest total surface area. When the fabric has a more surface area, there will be more contact area of the fabric and affecting higher the output performance of TENG. This effect was also reported in different materials from searching literature. Siju Mishra *et al.* [31] have investigated the potential application of surface-modified aluminum foils using commercially available emery papers. TENG based on surface-modified Al substrates has shown higher triboelectric performances of 138.1 V and 27.78 μA which was around 2.4 times and 2.5 times greater than plane Al foil. The combination of these line patterns increases the contact area between triboelectric materials which in turn boosted the output performance. Guo and co-workers [32] also demonstrated a high-performance fabric-based TENG by using a nylon cloth as the substrate and fluoroalkyl silane by the

chemically modified surface. The addition of a fluoroalkyl silane layer increases the surface area of the fabric based TENG resulting in increased output voltage and current from 53.2 V to 575 V and 1.1 μA to 12.1 μA as compared to the device without the fluoroalkyl silane layer. Thus, the result in this work can also fully confirm the significance of surface area of materials that influences the electrical output performance of the TENG device.

The output power of all fabrics under resistance conditions from 100 Ω to 10 M Ω was also investigated and shown in Figure 6(a-d).

It was also found that the maximum output power of rayon fabric for 53 μW at 1 M Ω resistance is higher than other fabrics at a resistance of 1 M Ω , as shown in Figure 6(c). This is because rayon fibers have a lengthwise striated surface and high surface area of fabric. The small-size fibers have more fibers per unit weight of the fabric, higher total fiber surface area, and greater possibilities for a charge to be generated with the fibers in the structure. This supports and allows rayon fibers to generate and exchange charges on the surface more than other fibers.

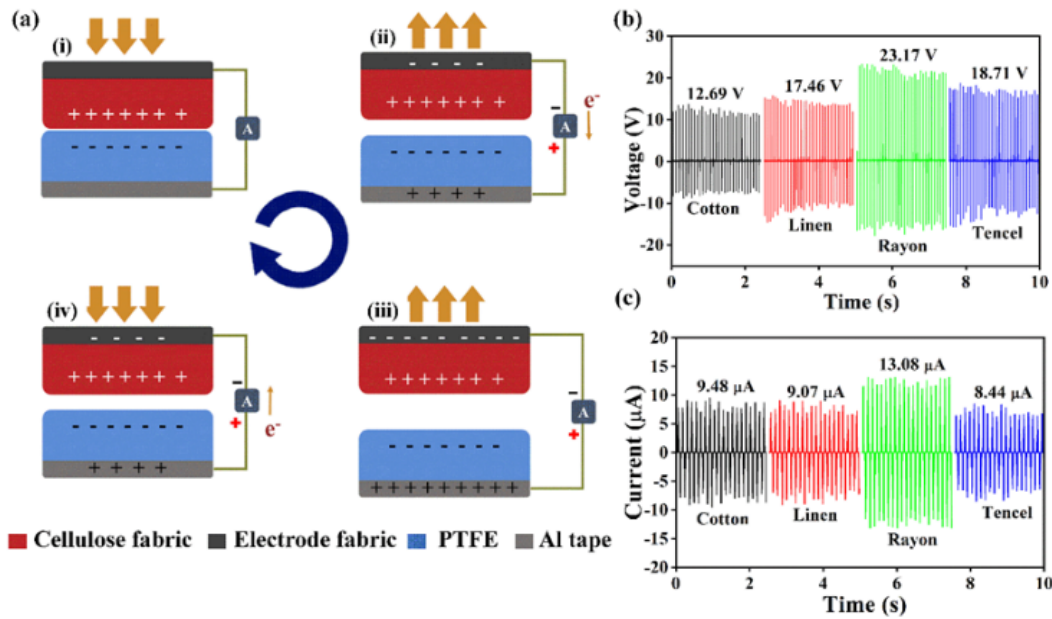


Figure 5. Electrical output of all fabrics. The working principle of the TENG device (a). The output voltage (b) and output current (c) of all fabrics.

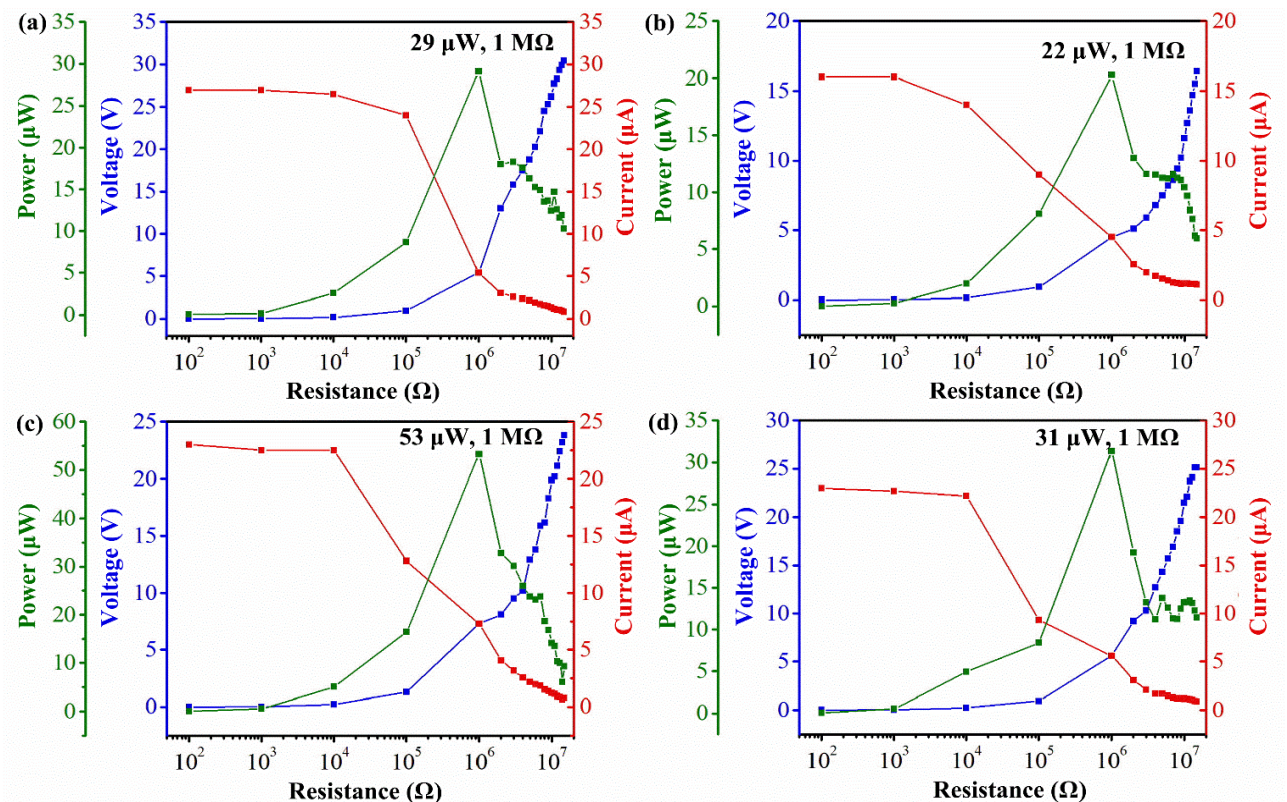


Figure 6. The maximum output power of cotton (a), linen (b), rayon (c), and tencel (d).

4. Conclusions

This research successfully fabricated textiles TENG using four types of commercial cellulose-based fabrics as friction layers to study the effects of different microstructures and surface area on output efficiency. The results confirm that even though rayon, linen, cotton and Tencel are the same types of cellulose molecule, the electric generation by meaning of TENG is totally different. The difference of output efficiency results by the different fiber diameters and surface area. Rayon fabric shows the smallest average diameter with highest surface area resulting in the highest output signal generation as compared to other fabrics. The investigation in this research confirms the importance of fiber characteristics in textile that influences directly to the TENG efficiency that helpful for the materials selection in the development of an efficient wearable electronic and wearable sensor using the TENG device.

Acknowledgements

This work of Thitirat Charoonsuk was supported financially by National Research Council of Thailand (NRCT) under the Grant Number N42A650220. The work of Satana Pongampai was funded by King Mongkut's Institute of Technology Ladkrabang with the Grant no. KREF146411 and the work of Naratip Vittayakorn was supported by KMITL under the Grant no. KREF116501.

References

- [1] K. R. S. D. Gunawardhana, N. D. Wanasekara, and R. D. I. G. Dharmasena, "Towards truly wearable systems: optimizing and scaling up wearable triboelectric nanogenerators," *iScience*, vol. 23, no. 8, pp. 101360, 2020.
- [2] S. Sriphan, and N. Vittayakorn, "Hybrid piezoelectric-triboelectric nanogenerators for flexible electronics: Recent advances and perspectives," *Journal of Science: Advanced Materials and Devices*, vol. 7, no. 3, p. 100461, 2022.
- [3] G. Zhu, B. Peng, J. Chen, Q. Jing, and Z. Lin Wang, "Triboelectric nanogenerators as a new energy technology: From fundamentals, devices, to applications," *Nano Energy*, vol. 14, pp. 126-138, 2015.
- [4] T. Charoonsuk, R. Muanghlua, S. Sriphan, S. Pongampai, and N. Vittayakorn, "Utilization of commodity thermoplastic polyethylene (PE) by enhanced sensing performance with liquid phase electrolyte for a flexible and transparent triboelectric tactile sensor," *Sustainable Materials and Technologies*, vol. 27, p. e00239, 2021.
- [5] D. G. Jeong, Y. J. Ko, J. H. Kim, D. S. Kong, Y. C. Hu, D. W. Lee, S. H. Im, J. Lee, M. S. Kim, G-H. Lee, C. W. Ahn, J. R. Ahn, N. Lee, J. Y. Park, and J. H. Jung, "On the origin of enhanced power output in ferroelectric polymer-based triboelectric nanogenerators: Role of dipole charge versus piezoelectric charge," *Nano Energy*, vol. 103, p. 107806, 2022.
- [6] S.-W. Kim, J.-K. Kim, H. J. Kim, C. T. Cao, N. Khen Oh, Y. Yang, H.-C. Song, M. Shim, H. S. Park, and J. M. Baik, "Output signals control of triboelectric nanogenerator with metal-dielectric-metal configuration through high resistance grounded systems," *Nano Energy*, vol. 95, p. 107023, 2022.
- [7] G. I. Dzhardimalieva, B. C. Yadav, T. Y. V. Lifintseva, and I. E. Uflyand, "Polymer chemistry underpinning materials for triboelectric nanogenerators (TENGs): Recent trends," *European Polymer Journal*, vol. 142, p. 110163, 2021.
- [8] D. Godwinraj, and S. C. George, "Recent advancement in TENG polymer structures and energy efficient charge control circuits," *Advanced Industrial and Engineering Polymer Research*, vol. 4, no. 1, pp. 1-8, 2021.
- [9] W. Paosangthong, M. Wagih, R. Torah, and S. Beeby, "Textile-based triboelectric nanogenerator with alternating positive and negative freestanding grating structure," *Nano Energy*, vol. 66, p. 104148, 2019.
- [10] P.-Y. Feng, Z. Xia, B. Sun, X. Jing, H. Li, X. Tao, H-Y. Mi, and Y. Liu, "Enhancing the performance of fabric-based triboelectric nanogenerators by structural and chemical modification," *ACS Applied Materials & Interfaces*, vol. 13, no. 14, pp. 16916-16927, 2021.
- [11] J. Xiong, P. Cui, X. Chen, J. Wang, K. Parida, M.-F. Lin, and P. S. Lee "Skin-touch-actuated textile-based triboelectric nanogenerator with black phosphorus for durable biomechanical energy harvesting," *Nature Communications*, vol. 9, no. 1, p. 4280, 2018.
- [12] H. J. Oh, J. H. Bae, J. Song, D. K. Kim, W. Lee, M. Kim, K. J. Heo, Y. Kim, S. H. Kim, B. J. Y, S. J. Lim, and Y. K. Park, "A highly porous nonwoven thermoplastic polyurethane/polypropylene-based triboelectric nanogenerator for energy harvesting by human walking," *Polymers*, vol. 12, no. 5, p. 1044, 2020.
- [13] J. Zhang, S. Hu, Z. Shi, Y. Wang, Y. Lei, J. Han, Y. Xiong, J. Sun, L. Zheng, Q. Sun, G. Yang, and Z. L. Wang, "Eco-friendly and recyclable all cellulose triboelectric nanogenerator and self-powered interactive interface," *Nano Energy*, vol. 89, p. 106354, 2021.
- [14] Z. Niu, W. Cheng, M. Cao, D. Wang, Q. Wang, J. Han, Y-Z Long, and G. Han, "Recent advances in cellulose-based flexible triboelectric nanogenerators," *Nano Energy*, vol. 87, p. 106175, 2021.
- [15] J. Jeong, "Comparative study of triboelectric nanogenerators with differently woven cotton textiles for wearable electronics," *Polymers*, vol. 11, no. 9, p. 1443, 2019.
- [16] L. Zhang, Y. Yu, G. P. Eyer, G. Suo, L. A. Kozik, M. Fairbanks, X. Wang, and T. Andrew, "All-textile triboelectric generator compatible with traditional textile process," *Advanced Materials Technologies*, vol. 1, no. 9, p. 1600147, 2016.
- [17] M. Sahu, S. Hajra, H.-G. Kim, H.-G. Rubahn, Y. Kumar Mishra, and H. J. Kim, "Additive manufacturing-based recycling of laboratory waste into energy harvesting device for self-powered applications," *Nano Energy*, vol. 88, p. 106255, 2021.
- [18] M. Zhu, Q. Shi, T. He, Z. Yi, Y. Ma, B. Yang, T. Chen, and C. Lee, "Self-powered and self-functional cotton sock using piezoelectric and triboelectric hybrid mechanism for healthcare and sports monitoring," *ACS Nano*, vol. 13, no. 2, pp. 1940-1952, 2019.

- [19] W. Sangkhun, and S. Wanwong, "Natural textile based triboelectric nanogenerators for efficient energy harvesting applications," *Nanoscale*, vol. 13, no. 4, pp. 2420-2428, 2021.
- [20] B. Dudem, A. R. Mule, H. R. Patnam, and J. S. Yu, "Wearable and durable triboelectric nanogenerators via polyaniline coated cotton textiles as a movement sensor and self-powered system," *Nano Energy*, vol. 55, pp. 305-315, 2019.
- [21] R. Xia, R. Zhang, Y. Jie, W. Zhao, X. Cao, and Z. Wang, "Natural cotton-based triboelectric nanogenerator as a self-powered system for efficient use of water and wind energy," *Nano Energy*, vol. 92, p. 106685, 2022.
- [22] R. Wu, L. Ma, A. Patil, Z. Meng, S. Liu, H. Chen, Y. Zhang, W. Yu, W. Guo, and X. Liu, "Graphene decorated carbonized cellulose fabric for physiological signal monitoring and energy harvesting," *Journal of Materials Chemistry A*, vol. 8, no. 25, pp. 12665-12673, 2020.
- [23] I. Jahan, "Effect of fabric structure on the mechanical properties of woven fabrics," *Advance Research in Textile Engineering*, vol. 2, no. 2, p. 1018, 2017.
- [24] F. Carrillo, X. Colom, J. J. Suñol, and J. Saurina, "Structural FTIR analysis and thermal characterisation of lyocell and viscose-type fibres," *European Polymer Journal*, vol. 40, no. 9, pp. 2229-2234, 2004.
- [25] M. L. Nelson, and R. T. O'Connor, "Relation of certain infrared bands to cellulose crystallinity and crystal latticed type. Part I. Spectra of lattice types I, II, III and of amorphous cellulose," *Journal of Applied Polymer Science*, vol. 8, no. 3, pp. 1311-1324, 1964.
- [26] E. Portella, D. Romanzini, C. Angrizani, S. Amico, and A. Zattera, "Influence of stacking sequence on the mechanical and dynamic mechanical properties of cotton/glass fiber reinforced polyester composites," *Materials Research*, vol. 19, no. 3, pp. 542-547, 2016.
- [27] F. Mizi, D. Dasong, and H. Biao, "Fourier transform infrared spectroscopy for natural fibres," in *Fourier Transform - Materials Analysis*, Rijeka: IntechOpen, 2012, pp.45-68.
- [28] I. R. Comnea-Stancu, K. Wieland, G. Ramer, A. Schwaighofer, and B. Lendl, "On the identification of rayon/viscose as a major fraction of microplastics in the marine environment: Discrimination between natural and manmade cellulosic fibers using fourier transform infrared spectroscopy," *Appl Spectrosc*, vol. 71, no. 5, pp. 939-950, 2017.
- [29] V. Somkuwar, A. Pragya, and B. Kumar, "Structurally engineered textile-based triboelectric nanogenerator for energy harvesting application," *Journal of Materials Science*, vol. 55, pp. 5177-5189, 2020.
- [30] F.-R. Fan, Z.-Q. Tian, and Z. Lin Wang, "Flexible triboelectric generator," *Nano Energy*, vol. 1, no. 2, pp. 328-334, 2012.
- [31] S. Mishra, P. Supraja, D. Haranath, R. R. Kumar, and S. Pola, "Effect of surface and contact points modification on the output performance of triboelectric nanogenerator," *Nano Energy*, vol. 104, p. 107964, 2022.
- [32] Y. Guo, K. Li, C. Hou, Y. Li, Q. Zhang, and H. Wang, "Fluoroalkylsilane-modified textile-based personal energy management device for multifunctional wearable applications," *ACS Applied Materials & Interfaces*, vol. 8, no. 7, pp. 4676-4683, 2016.